DOI: 10.1002/cbic.201000568

Engineering an Allosteric Binding Site for Aminoglycosides into TEM1-β-Lactamase

Alexander N. Volkov,[a, d] Humberto Barrios,[a] Pascale Mathonet,[a] Christine Evrard,[b] Marcellus Ubbink,[c] Jean-Paul Declercq,[b] Patrice Soumillion,*[a] and Jacques Fastrez*[a]

Allosteric regulation of enzyme activity is a remarkable property of many biological catalysts. Up till now, engineering an allosteric regulation into native, unregulated enzymes has been achieved by the creation of hybrid proteins in which a natural receptor, whose conformation is controlled by ligand binding, is inserted into an enzyme structure. Here, we describe a monomeric enzyme, TEM1-β-lactamase, that features an allosteric aminoglycoside binding site created de novo by directed-evolution methods. β-Lactamases are highly efficient enzymes involved in the resistance of bacteria against β-lactam antibiotics, such as penicillin. Aminoglycosides constitute another class of antibiotics that prevent bacterial protein synthesis, and are neither substrates nor ligands of the native β-lactamases. Here we show that the engineered enzyme is regulated by the binding of kanamycin and other aminoglycosides. Kinetic and structural analyses indicate that the activation mechanism involves expulsion of an inhibitor that binds to an additional, fortuitous site on the engineered protein. These analyses also led to the defining of conditions that allowed an aminoglycoside to be detected at low concentration.

Introduction

Enzymes, biological catalysts developed over the course of evolution, have a few fundamental characteristics in common: they transform their substrates with very high efficiency; most of them act specifically on a limited set of substrates; and a significant proportion of them are regulated by binding of ligands, "allosteric effectors", whose structures are different from those of their enzymes' substrates. With few exceptions, natural allosteric enzymes are oligomeric assemblies that consist of several subunits. Binding of allosteric effectors appears to induce changes in the interactions between the subunits and, as a consequence, conformational changes in the region of the active site; this leads to an increase or a reduction in substrate affinity or catalytic activity. Various allosteric control mechanisms have been proposed or discovered,[1,2] and a range of techniques has been used to discover allosteric communication pathways between active sites and regulatory sites within proteins.[3–5] A few monomeric enzymes have also been shown to be regulated by allosteric effectors. Natural effectors have been shown to activate a ribonucleotide reductase, and to modulate the specificity of a glucokinase, and their allosteric sites have been documented by crystallographic investigations.[6,7]

Despite the continuing improvement in our understanding of the mechanisms of allostery, the engineering of allosteric regulation remains a challenge. De novo creation of allosteric binding sites was first achieved by the insertion of known epitopes of monoclonal antibodies into the loops bordering the active site. Binding of the antibodies inhibited or mildly activated the engineered enzymes.[8–10] This approach was used to develop novel bioanalytical tools.[11] A generalization of the strategy (that bypassed the requirement for information about the epitopes) was established later by introducing phage-displayed libraries of mimotopes (epitope mimics) into the surface loops, and by selecting enzymes that bound to monoclonal antibodies through these mimotopes.[12] Indirect activation could be brought about by competitive binding of the hapten to the cavity of the antibody, thus reversing its inhibitory effect.

However, this approach cannot be easily applied to engineer regulation by small molecules; in this case, activation by induction of a conformational change, or expulsion of an enzyme-bound inhibitor could prove to be more viable strategies. The former was achieved by the creation of libraries of fusion pro-

[a] Dr. A. N. Volkov,[+] Dr. H. Barrios,[+] Dr. P. Mathonet,[+] Prof. P. Soumillion, Prof. J. Fastrez
Laboratoire d'Ingénierie des Protéines et des Peptides
Institut des Sciences de la Vie, Université Catholique de Louvain
Croix du Sud 4–5, Boîte 3, 1348 Louvain-la-Neuve (Belgium.)
Fax: (+32) 10-472820
E-mail: patrice.soumillion@uclouvain.be
jacques.fastrez@uclouvain.be

[b] Dr. C. Evrard, Prof. J.-P. Declercq
Unit of Structural Chemistry (CSTR), Université Catholique de Louvain
Place L. Pasteur 1, 1348 Louvain-la-Neuve (Belgium)

[c] Prof. M. Ubbink
Leiden Institute of Chemistry, Leiden University
Gorlaeus Laboratories
P.O. Box 9502, 2300 RA Leiden (The Netherlands)

[d] Dr. A. N. Volkov[+]
Present address: Jean Jeener NMR Center
Structural Biology Brussels, Vrije Universiteit Brussel
Department of Molecular and Cellular Interactions, VUB-VIB
Pleinlaan 2, 1050 Brussels (Belgium)

[+] These authors contributed equally to this work.

Supporting information for this article is available on the WWW under http://dx.doi.org/10.1002/cbic.201000568.

teins, in which β-lactamase was inserted randomly within the sequence of periplasmic maltose binding protein (MBP). Subsequent screening identified insertants whose activity could be switched on as a consequence of the natural conformational change induced in the MBP upon binding of its cognate ligand. Impressive activation factors were observed, and the activation itself was used for changing the nature of the activator (from maltose to sucrose) by a simple in vivo selection strategy.[13] Conversely, when the haem binding domain of cytochrome b_{562} was inserted randomly into the TEM1-β-lactamase, the activity could be inhibited or activated by haem binding.[14]

The construction of small-molecule-activated inteins, that is, autosplicing proteins, was achieved by using similar strategies.[15,16] The engineering of a light-dependent enzyme was carried out by insertion of a light-sensing signalling domain into a region of the enzyme that corresponded to an allosteric communication pathway.[17] In all these cases, the activity-controlling device was a natural protein domain, whose conformation depended on an inducing event. These strategies have been extensively reviewed recently.[18]

Here, we report the de novo engineering, by a directed evolution strategy, of an allosteric binding-site for aminoglycosides in a monomeric enzyme, TEM1-β-lactamase. β-Lactamases are enzymes involved in the resistance of bacteria against β-lactam antibiotics, which they hydrolyse very efficiently.[19] TEM1-β-lactamase was chosen as it had been engineered for regulation by the strategies mentioned above, which would allow comparison, and because it has been reported to support a very robust reporter activity.[20] Furthermore, compared to antibodies it is much easier to express in high yield. Aminoglycosides constitute another class of antibiotics that bind to the 30S subunit of bacterial ribosomes, and thus stall protein synthesis.[21] Aminoglycosides have been used extensively by veterinary practitioners, and their presence in foodstuffs is a growing source of concern, and hence must be monitored.[22,23] Furthermore, as they are rather hydrophilic compounds, it is unlikely they would bind to the enzyme primarily by nonspecific hydrophobic interactions. We show that this enzyme is activated by the binding of aminoglycosides. We have solved the crystal structure of the free protein, and have performed a solution NMR study of its interaction with kanamycin. Overall, kinetic and structural analyses indicate that the activation mechanism involves expulsion of an inhibitor that binds to an additional, fortuitous site on the engineered enzyme.

Results

Selection of a kanamycin-binding mutant

A library of phage-displayed mutants of TEM1-β-lactamase was used in the selection experiments designed to find kanamycin-binding mutants. In this library, random peptide sequences had been inserted in loops between the N- and C-terminal helices and their adjacent β-strands, and three residues in a loop connecting two β-strands bordering the active site had been randomized.[24] It was subjected to several rounds of bio-panning on immobilized biotinylated kanamycin A (KanA, Scheme 1), then to screening for the effects of KanA on activity. Error-prone PCR was then applied to improve these effects.

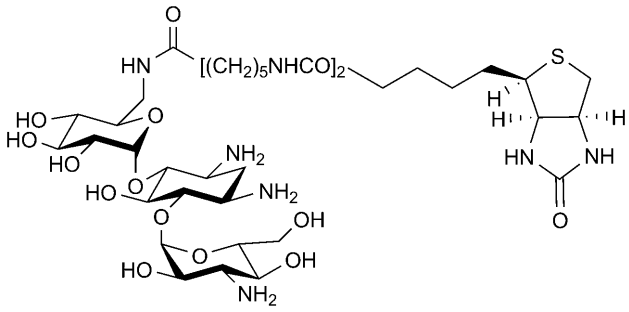

Scheme 1. Structure of biotinylated kanamycin A used for the selection of KanA binding β-lactamase variants from libraries.

The selected KanA-binding enzyme ("BlaKr", kanamycin-binding β-lactamase) was expressed in, and purified from *Escherichia coli*.

BlaKr contains the following modifications when compared to the wild-type enzyme: a six-residue extension (RTSHRP) flanked by cysteines, which replaced G41–A42 in loop L2 (connecting the N-terminal helix to the first β-strand); an E240R mutation in the G238 E240 R241 loop bordering the active site; and Q269R/A270K/T271K/M272T replacements in L1, the loop that connects the last β-strand to the C-terminal helix (Figure 1). An additional mutation, E104K, frequently found in extended-spectrum β-lactamases,[25] was also selected. In this paper, we follow the residue-numbering scheme of Ambler et al.,[26] and use alphanumeric notation for the inserted residues (C41-R41a-T41b-S41c-H41d-R41e-P41f-C42). Analytical size-exclusion chromatography indicated that BlaKr exists in a single, monomeric form at the concentration used for the analysis (~10 μM), and does not undergo oligomerization or domain swapping, as frequently observed when loops are mutagenized.[27]

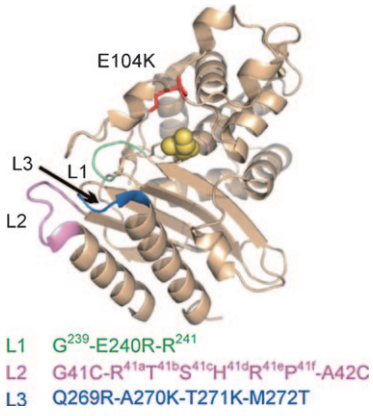

Figure 1. Crystal structure of BlaKr. The engineered loops are highlighted; the E104K point mutation is shown as sticks; the S70 active site is space-filled. The amino acid sequences of the engineered loops are given below.

Effect of ligands on BlaKr activity

The effect of KanA on BlaKr activity was initially monitored by following the decrease in UV absorbance upon benzylpenicillin ("PenG", penicillin G) hydrolysis at different KanA concentrations in MES (2-(*N*-morpholino)ethanesulfonic acid) buffer. A clear activation effect of KanA was observed (Figure 2). Experiments were then run at different pHs and in different buffers to better characterize the enzyme. A very puzzling observation was made: activation was observed only in aminosulfonic acid buffers. In order to clarify the activation mechanism, kinetic parameters were determined at various concentrations of MES and KanA in bis-tris buffer. Plots of k_{cat}, K_m, and k_{cat}/K_m as a function of [KanA] at high MES concentration are shown in Figure 3A. The increased catalytic efficiency (k_{cat}/K_m) in the presence of KanA appears to result mainly from a decrease in K_m, with only a modest effect detected on k_{cat}. As shown in Figure 3B, in absence of KanA, K_m increases linearly with [MES], which indicates that MES behaves as a competitive inhibitor. On the other hand, at saturation of KanA, K_m varies only slightly. These observations are compatible with a mechanism in which KanA activates the enzyme by expulsing MES, as formalized in the following kinetic model (Scheme 2).

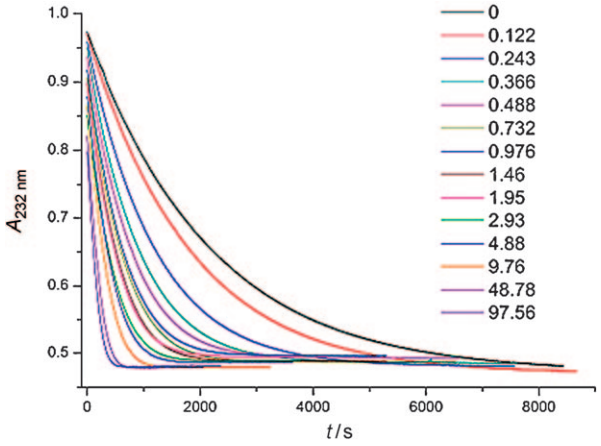

Figure 2. Effect of increasing the concentration of KanA on BlaKr-catalysed PenG hydrolysis detected by the change in UV absorbance ($\lambda = 232$ nm) at 30 °C in MES (20 mM, pH 6.6) and BlaKr (1.2 nM). KanA concentrations are given in μM in the inset.

The experimental values of k_{cat} and K_m obtained at various concentrations of MES and KanA were used to extract the k^0_{cat} and k^A_{cat}, K^0_m and K^A_m, $K_{d,E}$ and $K_{d,ES}$, and K^0_I and K^A_I parameters (see the Experimental Section), where the "0" and "A" superscripts correspond to absence and saturation in aminoglycoside, respectively. ("A" stands for aminoglycoside or activator.) $K_{d,E}$ and $K_{d,ES}$ represent the affinity of KanA for the free enzyme and the enzyme–substrate complex, respectively (Table 1). Sim-

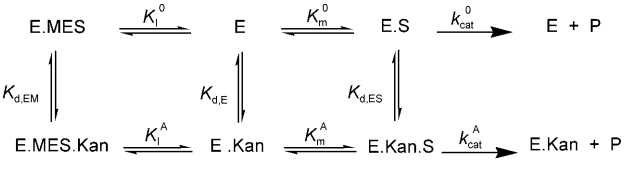

Scheme 2. Kinetic model proposed to explain the activation of the enzyme BlaKr by kanamycin-binding in MES buffer.

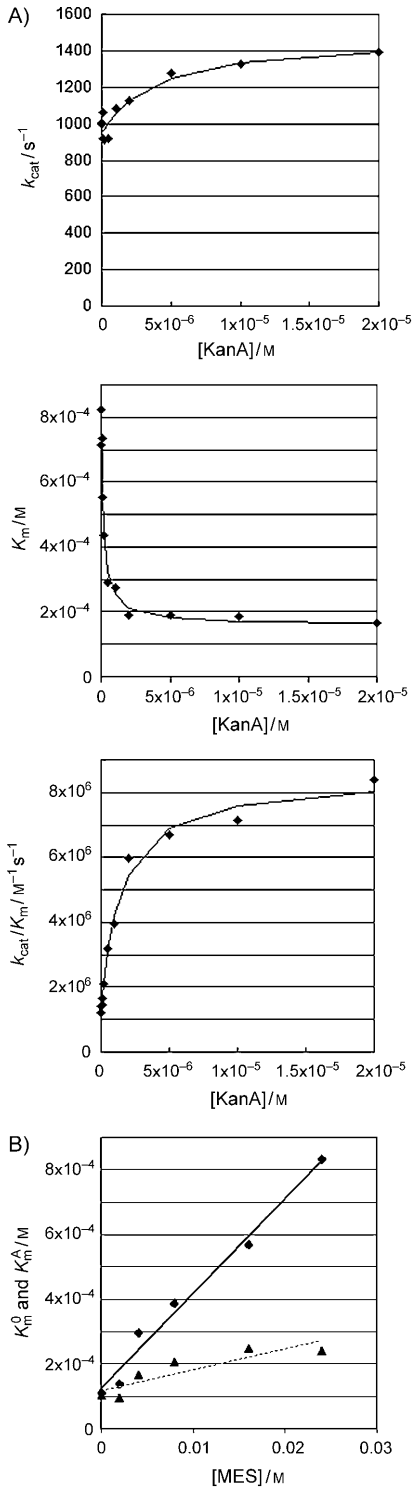

Figure 3. Kinetic analysis of BlaKr activation. A) Effect of increasing concentrations of KanA on the kinetic parameters k_{cat}, K_m and k_{cat}/K_m of PenG hydrolysis at 25 °C catalysed by BlaKr at pH 6.3 in MES/bis-tris mixed buffer (24 mM each). B) Effect of increasing concentrations of MES on the $K^0_{m,app}$ (◆) and $K^A_{m,app}$ (▲). The lines are best linear fits of the data.

Table 1. Kinetic parameters for the hydrolysis of PenG catalysed by BlaKr in the presence of MES and KanA[a]

k_{cat}^0	$820 \pm 140\ s^{-1}$	k_{cat}^A	$1220 \pm 160\ s^{-1}$
K_m^0	$(0.93 \pm 0.11) \times 10^{-4}$ M	K_m^A	$(1.00 \pm 0.13) \times 10^{-4}$ M
$K_{d,ES}$	$(2.6 \pm 1.6) \times 10^{-7}$ M	$K_{d,E}$[b]	2.4×10^{-7} M
K_I^0	$(3.0 \pm 0.4) \times 10^{-3}$ M	K_I^A	$(2.3 \pm 0.8) \times 10^{-2}$ M

[a] In bis-tris buffer (25 mM, pH 6.3), MES added at concentrations between 0 and 25 mM. [b] $K_{d,E}$ is calculated from the thermodynamic cycle of Scheme 1.

Table 3. Inhibition constants of aminosulfonic acids in bis-tris buffer (pH 6.3).

Aminosulfonic acid	K_I^0 [M]	K_I^{KanA} [M]
taurine	0.008 ± 0.004	0.06 ± 0.03
MES	0.003 ± 0.00044	0.023 ± 0.008
BES	0.0007 ± 0.0001	0.01 ± 0.0025
MOPS	0.013 ± 0.004	0.024 ± 0.005

ilar experiments, performed with the wild-type enzyme as a control, showed no significant inhibition by MES, and no activation by KanA.

The enzyme appears to have acquired two physically or functionally overlapping binding sites: a low affinity one for MES, and a high affinity one for KanA. Analogous kinetic analyses with various aminoglycosides (Scheme 3A) and aminosulfonates (Scheme 3B) documented the specificity of both binding sites (Tables 2 and 3). KanA was not the aminoglycoside ligand with the highest affinity. Kanamycin B and tobramycin, whose structures are similar, bound with approximately fivefold-higher affinity. Isepamicin and ribostamycin, whose structures are different, bound with slightly lower affinity. A comparison of the $K_{m,app}^A$ or $(k_{cat}/K_m)_{app}^A$ values suggests that the last two aminoglycosides might be less efficient at expelling MES. The submicromolar affinities of the first three aminoglycosides are not very different from the affinities of monoclonal antibodies for kanamycin (20–40 nM), as calculated from the data of Watanabe[22] or Loomans.[23] Affinities for oligosaccharides or similar compounds are rarely in the nanomolar range, because the hydrogen bonds contributing to binding are solvated by water in the free protein and ligand.[28,29]

Table 2. Binding constants of aminoglycosides in 24 mM MES buffer at pH 6.3.

Aminoglycoside	k_{cat}^A [s^{-1}]	$K_{m,app}^A$ [mM]	$(k_{cat}/K_m)_{app}^A$ [$M^{-1}s^{-1}$]	$K_{d,ES}$ [μM]
isepamicin	1316 ± 357	0.28 ± 0.14	$(4.6 \pm 0.2) \times 10^6$	0.45 ± 0.11
kanamycin A	1481 ± 221	0.16 ± 0.08	$(8.5 \pm 0.7) \times 10^6$	0.17 ± 0.02
kanamycin B	1328 ± 116	0.18 ± 0.03	$(7.8 \pm 0.6) \times 10^6$	0.045 ± 0.004
ribostamycin	1430 ± 210	0.26 ± 0.09	$(6.2 \pm 0.5) \times 10^6$	0.30 ± 0.08
tobramycin	1113 ± 68	0.14 ± 0.02	$(8.7 \pm 0.3) \times 10^6$	0.031 ± 0.011

As far as the aminosulfonic acids are concerned, BES is a better inhibitor than MES, which is in turn superior to taurine. MOPS, which contains an additional methylene group between the amine and the sulfonate moieties, appears to fit less tightly in its binding site (Table 3). Some aminosulfonate binding was still detected at saturation in KanA (the observed $K_{m,app}^A$ does not extrapolate back to K_m^0, i.e., 0.09 mM); this indicates that the aminoglycosides are not fully competitive with the aminosulfonic acids. The ratio of binding constants (K_I^0 versus K_I^A) is approximately ten except again for MOPS, which seems to be less efficiently expelled by KanA. Surprisingly, the low-affinity aminosulfonate binding-site appears to be more specific than the aminoglycoside site.

The effects of MES and BES on the hydrolysis of PenG and nitrocefin (a larger, chromogenic β-lactamase substrate) were also measured by following full-progress curves. The K_I^0 values obtained with nitrocefin were similar to those reported for PenG. However, the value of k_{cat}/K_m extrapolated to saturation in MES does not tend to zero but to $26 \pm 5\%$. By comparison, BES inhibited nitrocefin hydrolysis nearly quantitatively, while taurine at 0.1 M hardly affected it at all. A small activity on PenG (~5%) remained in 0.1 M MES, and none in 0.1 M BES.

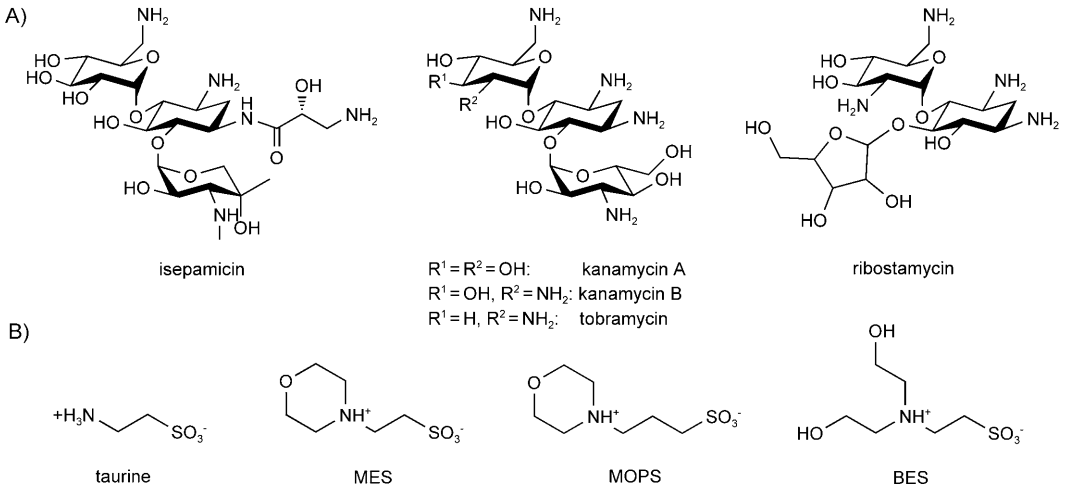

Scheme 3. Structures of the ligands binding to the enzyme BlaKr, and tested in this work: A) aminoglycosides; B) aminosulfonic acids.

The effect of tobramycin on nitrocefin hydrolysis in 25 mM BES buffer started to be detected in the 100 nM concentration range (Figure 4) while BlaKr-specific activity increased more than 25-fold between 10 nM and 10 μM tobramycin. For food safety regulations, the maximum tolerated concentration of aminoglycosides in milk is of the order of 300 nM.[30] For practical applications, however, additional work would be needed to eliminate potential interactions with other components in milk.

In addition to the ligands described above, negatively charged heparin fragments (disaccharide I-S, disaccharide II-H, disaccharide III-H), and glucosamine have been tested for their effect on BlaKr activity at concentrations ranging from 0 to 100 μM. None of them affected the activity.

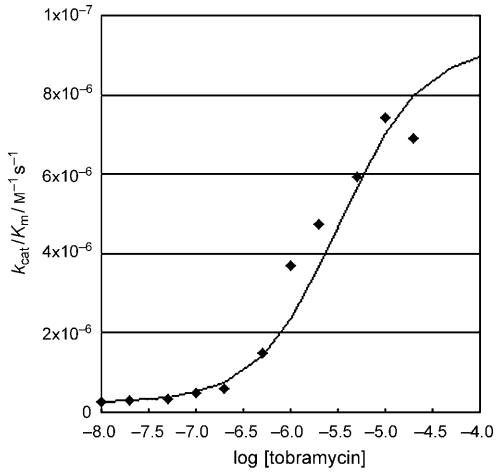

Figure 4. Effect of increasing concentration of tobramycin on the hydrolysis of nitrocefin. Full hydrolysis curves of 5 μM nitrocefin in the presence of 20 nM BlaKr and various concentrations of tobramycin followed at 482 nm in BES (25 mM, pH 6.6, 25 °C). The k_{cat}/K_m parameters were obtained by dividing the derived first order rate constants k_{obs} by the BlaKr concentration.

Isotermal titration calorimetry (ITC)

ITC experiments were also performed, in order to assess MES and KanA binding to BlaKr by an independent method. Binding of phenethylboronic acid (PhBA), a transition-state analogue and competitive inhibitor of wild-type β-lactamase (wt Bla),[31] was used as a reference. The binding parameters presented in Table 4 were obtained from titration curves that used a 1:1 binding model (see Figure S1 in the Supporting Information). The interaction stoichiometry appears to deviate significantly from unity. At this stage we do not have a satisfactory explanation for this observation. KanA binds to BlaKr in both MES and cacodylate buffer, while no binding is detected in phosphate buffer. A comparison of the apparent KanA binding constants to BlaKr or the BlaKr–PhBA complex in MES buffer ($K_d = 24$ and 41 μM, respectively) indicates that these two interactions are independent.

Table 4. ITC binding parameters for BlaKr (0.7–1.5 mM) with different buffers (20 mM, pH 6.6, 30 °C).

Interaction	Buffer	N[a]	K_d [μM]	ΔG_B [kJ mol^{-1}]	ΔH_B [kJ mol^{-1}]	$-T\Delta S_B$ [kJ mol^{-1}]
BlaKr + KanA	MES (4)[b]	0.6 ± 0.1	24 ± 1	−26.9 ± 0.1	−9.6 ± 0.4	−17.1 ± 0.4
	cacodylate (3)[b]	0.8 ± 0.1	51 ± 2	−25.1 ± 0.1	−20.1 ± 2.1	−5.0 ± 2.1
	phosphate (3)[b]	–	n.d.[c]	–	≈0	
BlaKr + PhBA	MES (2)[b]	0.7 ± 0.1	100 ± 6	−23.3 ± 0.2	−63.9 ± 6.7	40.6 ± 7.1
BlaKr-PhBA + KanA	MES (3)[b]	0.6 ± 0.1	41 ± 3	−25.6 ± 0.2	−3.8 ± 1.3	−21.3 ± 1.3

[a] Binding stoichiometry. [b] Number of titrations performed. [c] Binding not detected.

Structural characterization

The crystal structure of free BlaKr was solved at 1.6 Å. The electron density was well defined along the protein chain, except for the C-terminal part of the molecules, where about 20 residues (including a His-tag) were not observed. Ramachandran plots show that more than 98% of the residues lie in favoured regions, and that all of them adopt an allowed conformation (for the refinement statistics see Table S2). The structure is similar to that of the wild-type protein,[32] except for the loop insertion (Figure 1). The cysteines bordering the loop following the N-terminal helix form a disulfide bridge.

Despite numerous attempts to diffuse KanA into BlaKr crystals, and to co-crystallize BlaKr–KanA in different buffers, we have not succeeded so far in solving the structure of the complex. A likely cause of this failure is crystal packing of the individual protein molecules; this partially occludes the putative KanA binding site. In a structure obtained during the co-crystallization attempts, two sulfate ions were found, one of which interacts with the side chain of R240 and the NH atom of R241 in the engineered loops region where MES binds (see below).

For the detection of kanamycin binding by NMR spectroscopy, a [U-^{13}C, U-^{15}N] BlaKr sample was prepared. Its 2D ^{1}H,^{15}N TROSY spectrum showed good peak dispersion in both proton and nitrogen dimensions. The backbone resonance assignments, derived from a suite of 3D TROSY-type NMR experiments (Experimental Section), were facilitated by the published chemical shifts for the wild-type protein.[33,34] In total, assignments were obtained for 96% of backbone ^{1}HN and ^{15}N (for all non-proline residues), 98% of all $^{13}C_\alpha$, 91% of all $^{13}C_\beta$ and 91% of all ^{13}C atoms. In addition to three residues (H26, S70, and A237), whose ^{1}HN/^{15}N resonances were also unassigned in wt Bla,[34] we could not assign the BlaKr backbone amides of T41b (part of the engineered loop), T272 (a point mutation), and five residues in K215–L221 stretch. Besides, weak peaks of S41c, M68, and R241—observed in the spectrum of BlaKr in sodium phosphate—disappeared in the spectrum acquired in MES. Overall, the BlaKr chemical shifts were in a good agreement with those for the wild-type protein,[34] except for the residues in and around the mutation sites. The chemical shifts are deposited in BioMagResBank (accession number BMRB 15917).

In order to define the binding sites of KanA, 2D NMR spectra of ^{15}N BlaKr in the presence of increasing amounts of KanA were acquired, and the binding-induced spectral changes analysed. In 20 mM sodium phosphate, the BlaKr spectrum remained unperturbed in the presence of up to fivefold excess of KanA (data not shown). When 20 mM MES was used instead of phosphate, addition of KanA led to chemical shift perturbations ($\Delta\delta$) of ^{1}HN and ^{15}N nuclei for some BlaKr residues (Figure 5A). Throughout the titration, a single set of resonances was observed at each KanA concentration, the binding shifts were proportional to the amount of KanA added, and the line widths remained constant. This indicates that the BlaKr–KanA interaction is in fast exchange on the NMR chemical-shift timescale, with an estimated dissociation rate constant $k_{off} \gg 130\ s^{-1}$. Changes in $\Delta\delta$ during the ^{15}N BlaKr–KanA titration, monitored in a series of spectra, fit well to a 1:1 binding model, with a shared K_d of 32 μM (Figure S2)—in agreement with the ITC-determined K_d (24 μM). For a comparison with the value obtained in the kinetic experiments, these apparent constants should be divided by $(1+[MES]/K^0_{MES})$. The corrected value (3.6 μM) is ten times higher than that derived from the kinetics analysis. However, the NMR and ITC values were obtained at very different protein concentrations (millimolar vs nanomolar) and slightly different pH and temperature; this could account for the discrepancy.

The binding shifts observed upon KanA addition to BlaKr in MES were small: maximum values were $\Delta\delta_H = 0.1$ ppm, $\Delta\delta_N = 0.3$ ppm and $\Delta\delta_{av} = 0.072$ for the weighted average, $\Delta\delta_{av} = \sqrt{((\Delta\delta_N/5)^2 + \Delta\delta_H^2)/2}$. Several regions of BlaKr were affected, for example the loops adjoining the N- and C-terminal α-helices and the areas encompassing residues T128–N132 and E166–D176 (Figure 5A). The chemical-shift perturbation map (Figure 5C) revealed a single binding patch on the surface of BlaKr, located around residues R41a–R41e (part of the engineered loop), I173–D176, and G267–K271 (mutations in the loop preceding the C-terminal helix). Interestingly, a number of buried amino acid residues—several of which sit close to or within the enzyme's active site (e.g., N132 and E166)—also exhibit significant $\Delta\delta_{av}$ (Figure 5C).

Upon titration with PhBA, a number of ^{15}N BlaKr resonances disappeared, and some reappeared elsewhere in spectra acquired at higher PhBA concentrations. Such behaviour indicates that the BlaKr–PhBA interaction is in slow exchange on the NMR chemical shift timescale; this necessitated the assignment of the backbone amide resonances of the bound form. Overall, the $\Delta\delta_{av}$ values for BlaKr–PhBA are much larger than those for BlaKr–KanA in MES, and the region affected by PhBA is different (Figure 5B). According to the chemical shift map (Figure 5D), PhBA docks to the substrate-binding pocket, and affects many residues in and around the enzyme's active site (as expected for a transition state analogue).

Discussion

From a library of phage-displayed β-lactamase variants, we have isolated an enzyme (BlaKr) that features an allosteric binding site for aminoglycosides, as was expected from the designed selection protocol. Surprisingly, an additional low-affinity binding-site for aminosulfonic acid was also detected in this enzyme. The evidence for aminoglycoside and aminosulfonic acid binding came from their effect on the kinetics of the hydrolysis of penicillin and cephalosporin substrates. Aminosulfonic acids inhibit the enzyme through an apparent competitive inhibition mechanism (effect on K_m); aminoglycosides appear to reactivate it by expulsion of the inhibitor. Conversely, the binding of aminosulfonic acids reduced the affinity of BlaKr for aminoglycosides. KanA binding was also observed by ITC except in phosphate buffer where no ITC signal was recorded, either because the ΔH_B is too small or because the affinity is much lower in this buffer. The absence of perturbation of the BlaKr spectrum by KanA-addition in phosphate buffer, and the high K_d value (~1 mM) recorded by measurements of the effect of KanA on rates of PenG hydrolysis in the same buffer, support the second hypothesis. The occurrence of a number of arginine residues in the engineered site might explain this behaviour as the guanidinium function is known to interact strongly with phosphate anions.[35]

BlaKr was nearly as active as TEM1-β-lactamase, which has been described as a perfect enzyme—that is, an enzyme whose activity is diffusion limited.[36] Its k_{cat} versus PenG was similar to that of the wild-type enzyme, and its K_m was only slightly larger (~two- to threefold). The insertion and mutations in loops close to the active site did not significantly degrade the activity. As a consequence, BlaKr could barely be activated directly by an allosteric ligand. By comparison, the creation of a hybrid protein (by insertion of the TEM1-β-lactamase into the MBP)[13] strongly deactivated the enzyme, and hence ligand-induced activation could be observed.

While BlaKr was extracted from a library in which random peptides had been inserted in two loops, an insertion was found only in loop L2 (Figure 1). The lack of any insertion in loop L3 might have resulted from its rare occurrence (~7%) in libraries selected for catalytic activity.[24]

The backbone amide chemical-shift perturbations observed in the NMR spectra on addition of KanA to BlaKr in MES buffer (Figure 5A) could have arisen from KanA binding, MES expulsion or a combination of both. A plot of the difference between the BlaKr spectra in phosphate or MES buffer versus the perturbations induced by Kan-binding in MES sheds some light on this question (Figure 6A). Nine residues with $\Delta\delta_{av.Kan}$ larger than twice the standard deviation above their mean, had very similar $\Delta\delta_{av.Kan}$ and $\Delta\delta_{av.phosphate} - \Delta\delta_{av.MES}$ values (filled diamonds). This strongly suggests that these shifts result from an identical cause: MES expulsion by Kan versus "phosphate in–MES out" in the difference spectrum. Besides these nine points, only three additional amide signals (filled squares) featured significant $\Delta\delta_{av.Kan}$ shifts; they are also significant on the $\Delta\delta_{av.phosphate} - \Delta\delta_{av.MES}$ axis. This scarcity, and the generally low perturbations on the $\Delta\delta_{av.Kan}$ axis provide far too few indications to position the aminoglycosides binding site.

Based on the results of the extensive kinetics analysis and the limited NMR data presented in this work, we would like to propose that although MES behaves kinetically as a competitive inhibitor, it does not bind to the active site. It is likely that

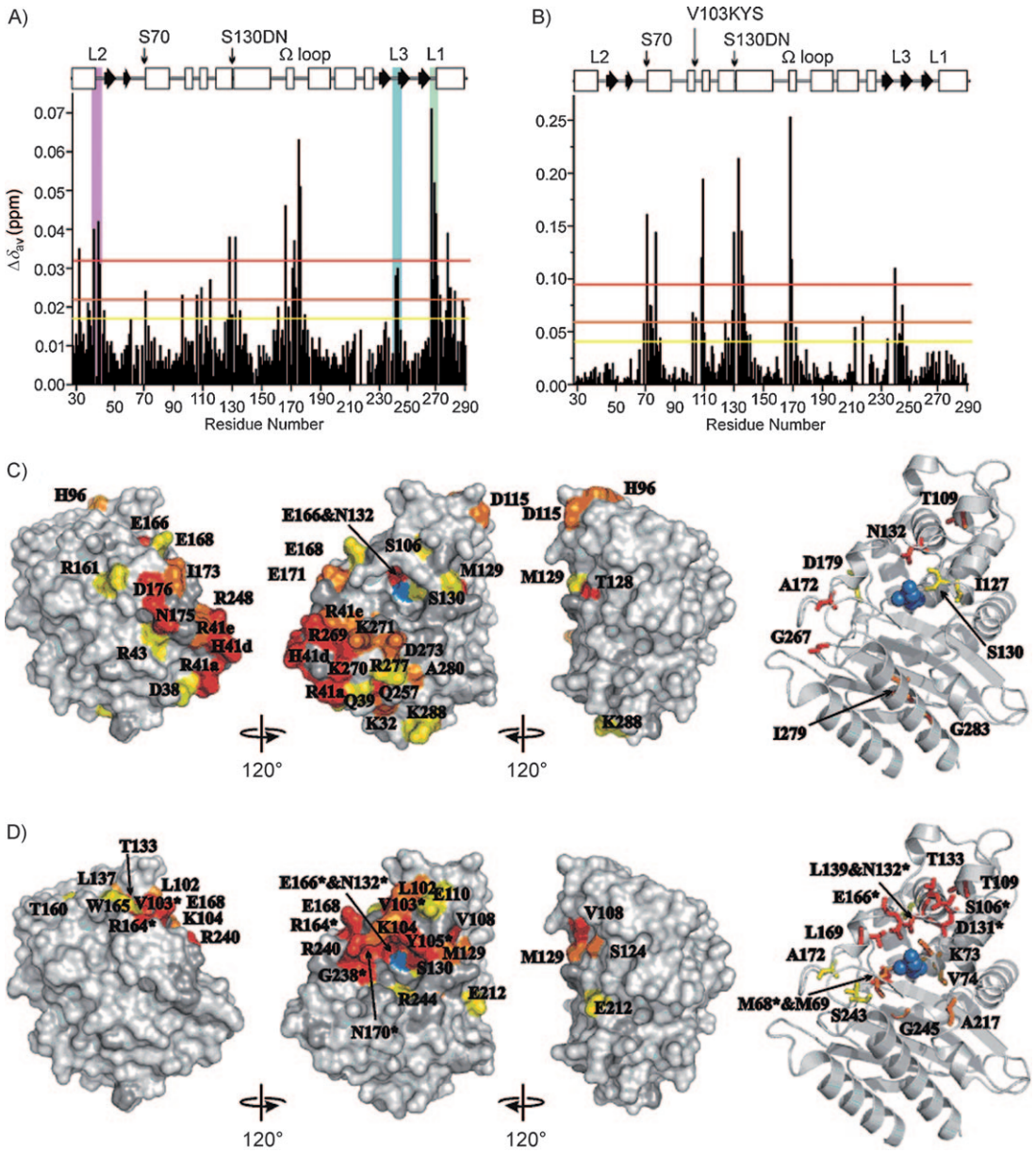

Figure 5. Chemical shift perturbation analysis of BlaKr binding to A) KanA and B) PhBA. These plots show averaged chemical shift perturbations ($\Delta\delta_{av}$) of BlaKr backbone amides ^{1}HN and ^{15}N nuclei in the presence of tenfold excess of KanA in MES, and fourfold excess of PhBA in sodium phosphate, respectively. In each plot the horizontal lines denote the significance levels equal to the mean $\langle\Delta\delta_{av}\rangle$ plus one-half, one, and two standard deviations (σ). The secondary structure of the protein is shown above, with α-helices (□) and β-strands (▶). Loop colouring (left panel) is as in Figure 1. BlaKr structures (PyMOL).[46] Effect of C) KanA and D) PhBA binding. Residues are coloured according to the $\Delta\delta_{av}$ significance level in (A) and (B): light cyan (unaffected residues with $\Delta\delta_{av} <$ mean $+ {}^{1}/_{2}\,\sigma$), yellow ($\Delta\delta_{av} >$ mean $+ {}^{1}/_{2}\,\sigma$), orange ($\Delta\delta_{av} >$ mean $+\,\sigma$), and red ($\Delta\delta_{av} >$ mean $+\,2\,\sigma$). Prolines and residues with unassigned backbone amide resonances are shown in grey, and the catalytic S70 is in blue. Labels identify BlaKr residues affected by binding. Buried residues are shown as sticks in the cartoon representations (right), with the catalytic S70 space-filled. In (D), asterisks point to residues whose resonances are broadened beyond detection upon binding of PhBA.

binding sites for aminosulfonic acids and substrates are contiguous but distinct, as shown by a comparison of the chemical-shifts perturbations arising from KanA-binding/MES-displacement with those induced by interaction with the active site ligand, PhBA.[31] The correlation coefficient of a plot of $\Delta\delta_{av,PhBA}$ versus $\Delta\delta_{av,kan}$ is close to zero (Figure 6B). However, MES binding induces a chemical shift in N132, a residue which interacts with the substrate side chain.[37] Hence, MES might reduce the affinity of the enzyme for its substrate by indirect competition for an anchor point. The significant level of activity that remained at saturation in MES, at least with nitrocefin as substrate, supports this interpretation.

Two mechanisms can be proposed to explain the functional competition between the BlaKr ligands: steric interaction, and an indirect effect by induction of conformational changes. TEM1-β-lactamase has been described, on the basis of an NMR investigation, as one of the most ordered proteins,[34] and the presence of a disulfide bridge in loop L2 is likely to increase

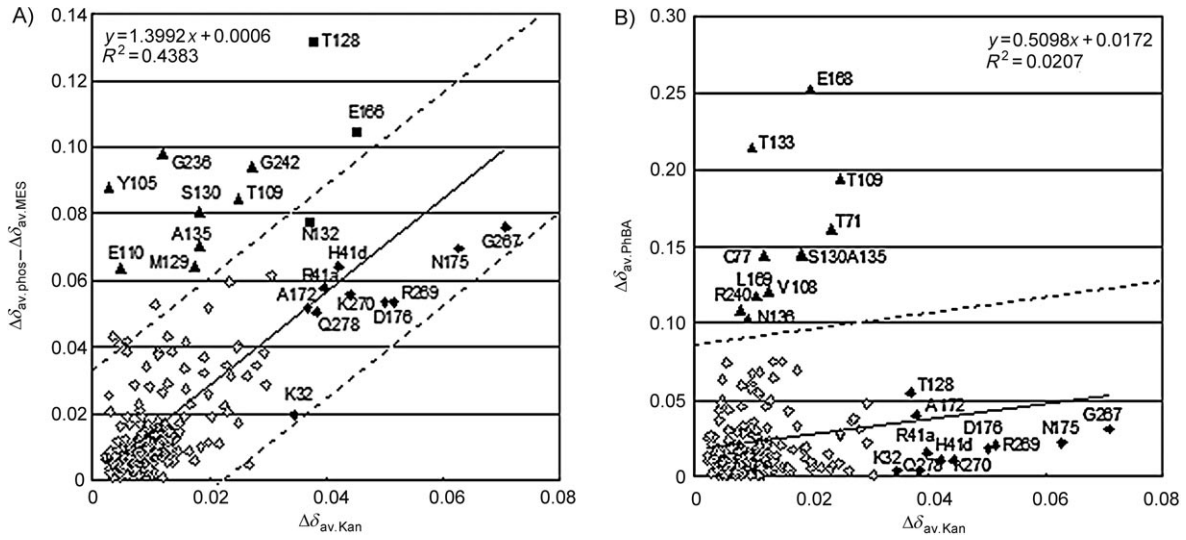

Figure 6. Chemical-shift maps of BlaKr in the presence of KanA or PhBA. Left pane: $\Delta\delta_{av}$ in phosphate$-\Delta\delta_{av}$ in MES buffers plotted versus averaged chemical-shift perturbation on titration of BlaKr with KanA in MES. Right pane: $\Delta\delta_{av,PhBA}$ plotted versus $\Delta\delta_{av,Kan}$. Residues whose $\Delta\delta_{av}$ exceed $\langle\Delta\delta_{av}\rangle$ by at least two σ are labelled and indicated by ◆ ($\Delta\delta_{av,Kan}$), ▲ ($\Delta\delta_{av,phosphate}-\Delta\delta_{av,MES}$) and ■ (both conditions). The continuous lines follows the linear correlation on all points; the parallel dotted lines are $2\sigma_{xy}$ above and below. All experiments were performed in 20 mM buffers, pH 6.6, at 30 °C.

BlaKr rigidity. This would favour a mechanism of steric interaction. However, several observations suggest that this enzyme is responsive to binding events relatively far from the active site. In hybrid proteins, in which ligand binding domains were associated with the TEM1-β-lactamase,[13, 14] conformational changes induced by binding were clearly transmitted to the enzyme and affected the activity. When variants of TEM1-β-lactamase (endowed with transition metal ions affinity) were selected from our insertant libraries, the binding of ions to histidine residues 15–20 Å from the active site activated or inhibited the enzyme.[38] The binding of ligands to a serendipitous allosteric site, 16 Å from the active site characterized by X-ray crystallography, was shown to inhibit the enzyme by "core disruption".[39] All these observations are more consistent with an interpretation of allosteric regulation, in which the binding of a ligand affects the relative free energies of protein states that differ in their affinities for other ligands.[40] Our observations fit better with this model. The size of the region perturbed by KanA-binding/MES-displacement is clearly larger than the ligands themselves: distances of 30 Å are found between the C_α atoms of R41b and N132 or E166 (residues belonging to the SDN motif and the Ω-loop important for β-lactamase activity).[19] Furthermore, a number of buried BlaKr residues are affected by KanA binding (Figure 5C), several of which (e.g., G267 and A172) sit close to the surface. Their chemical-shift perturbations cannot be attributed to direct interactions with a ligand, but rather result from secondary effects, such as rearrangements of protein side chains or local backbone movement. Binding of aminoglycosides, on the other hand, does not shift the enzyme conformation to a less active state, possibly because (being hydrophilic) they do not lead to "core disruption".

In conclusion, we show here that several binding sites can coexist on a monomeric enzyme. This might be a general property of natural proteins, as shown by the results of recent high-throughput screening programs for drug discovery and crystallographic analyses that led to the serendipitous detection of many allosteric sites.[41] Components of crystallization media are also frequently found by chance in protein cavities. We show also that a directed-evolution strategy can be used successfully to introduce an allosteric site onto an enzyme framework without impairing its activity. Interactions of the allosteric ligands with the enzyme (or among them) might lead to a modulation of function, that is, enzymatic activity. This suggests that there is an opportunity for designing molecular biosensors by engineering allosteric regulation functions. However, harnessing this property remains a challenge, and will require the design of more sophisticated selection protocols.

Experimental Section

Materials: Kanamycin A disulfate was purchased from Riedel-de Haën or Roche (NMR experiments). Ribostamycin sulfate, tobramycin, and heparin fragments (disaccharide I-S, disaccharide II-H, disaccharide III-H), phenethylboronic acid and the buffers (Biotechnology Performance Certified), MES, BES, MOPS and bis-tris were purchased from Sigma–Aldrich. Glucosamine hydrochloride, kanamycin B sulfate and taurine (Bioultra) were purchased from Fluka.

Selection of BlaKr clone: Biopanning experiments were performed in TBS (Tris buffer saline: 50 mM Tris.HCl, 150 mM NaCl, pH 7.5) on freshly prepared phages by using previously described phage libraries[21] and protocols[12] with minor modifications. The following supports were used: streptavidin Dynabeads M-270 (Dynal) and avidin-coupled agarose (Sigma), each presaturated for one hour with biotinylated kanamycin (50 μM in TBS containing 0.1% milk protein (M-TBS)). Two buffers were used to block nonspecific sites: M-TBS and G-TBS (TBS containing EIA grade gelatine (1% (*w*/*v*); BioRad)). For the first two rounds of selection, elutions were performed by competition with 100 μM KanA; this was dialysed

before infection of the bacterial culture by the eluted phages to prevent its inhibition. From the third round, elution was performed by trypsin cleavage (200 nM, 20 min) of the connector between the enzyme and the phage g3p protein. Elution yields after six rounds remained in the 10^{-5} range. DNA sequencing of 36 clones, picked randomly after six rounds of selection, pointed to consensus sequences, but ELISA tests did not give clear positive signals. Individual clones were screened to detect the effect of KanA on their hydrolytic activity on PenG. A phage–enzyme complex was found that showed a weak (~40%) increase in activity in phosphate buffer (apparent affinity $K_d = 0.66 \pm 0.09$ mM). This clone featured the following sequence in the loops: C41-R41a-T41b-S41c-H41d-R41e-P41f-C42, G238-R240-R241, R269-K270-K271. In view of its low KanA affinity, it was not studied in more detail, but it was subjected to a cycle of error-prone PCR, and the second-generation library was selected by five further rounds of biopanning on alternating supports as above. The number of washes was increased as selection progressed; elution was performed by competition with 100 μM KanA. Phages isolated by affinity selection were additionally selected for β-lactamase activity by spreading bacterial cells infected with selected phages on plates containing ampicillin (20 mg L^{-1}, overnight incubation at 30 °C). Twenty clones were sequenced and subjected to screening for their effects under increasing concentrations of KanA in MES buffer. The clone displaying the largest effect ("BlaKr") was chosen for further studies. It featured two additional mutations: E104K and M272T.

Preparation of BlaKr samples: The gene coding for BlaKr was cloned into a pET24(ompA) expression plasmid,[42] downstream of the OmpA signal peptide, and into a vector derived from pBAD/*Myc*-His (Invitrogen) to express the protein either extracellularly or intracellularly, free or in fusion with a His-tag, respectively. It was purified by following published procedures.[24,34,42] Uniformly labelled ^{15}N and ^{13}C proteins were produced in M9 minimal medium with $^{15}NH_4Cl$ (99% pure, Cambridge Isotope Laboratories) and $^{13}C_6$-D-glucose (99% pure, CortecNet, Paris) as sole nitrogen and sugar sources. Protein concentrations were determined from UV/Vis spectra by using a calculated[43] value of the extinction coefficient, $\varepsilon_{280} = 28.21$ mM $^{-1}$ cm $^{-1}$.

Kinetics: BlaKr-catalysed hydrolysis was followed by the decrease in UV absorbance of the PenG substrate at 232 nm ($\Delta\varepsilon = 1040$ M $^{-1}$ cm $^{-1}$) or, for solutions containing bis-tris (25 mM) at 239 nm ($\Delta\varepsilon = 689$ M $^{-1}$ cm $^{-1}$). PenG (100 μL) and aminoglycoside (10 μL) were added to buffer (2 mL, aminosulfonic acids or bis-tris containing aminosulfonic acids at various concentrations) and equilibriated at 25°. Then stock enzyme solutions (10 μL, from 500 nM to 1 μM, containing 10 μM BSA) were added. The k_{cat}^{obs} and K_m^{obs} parameters were calculated from the initial rate constants k_{obs}, measured at several substrate concentrations; they were estimated to within 10 and 20% fluctuations, respectively, in independent experiments. These parameters were plotted as functions of aminoglycoside concentration, and the $k_{cat,app}^0$, $k_{cat,app}^A$, $K_{m,app}^0$ and $K_{m,app}^A$ values were determined by nonlinear regression on k_{cat}^{obs} and K_m^{obs} weighted by their 95% confidence limits. For the KanA–MES system, the true parameters K_m^0, K_m^A, k_{cat}^0/K_m^0, k_{cat}^A/K_m^0, $K_{d.ES}$ and $K_{d.E}$ (as defined in Scheme 1 and Table S1) were obtained by fitting 72 k_{cat}^{obs} and K_m^{obs} value pairs obtained at various concentrations of these ligands. As the influence of the aminoglycoside concentration on k_{cat} is small, these parameters were not used to determine $K_{d.ES}$. K_I values for the aminosulfonates (Table 3) were estimated from the ratios of $K_{m,app}^0$ to $K_{m,app}^A$ obtained at 24 mM, and in their absence, obtained at eight concentrations of kanamycin A (between 0 and 20 μM). The $K_{d.ES}$ values for the aminoglycosides (Table 2) were estimated from $K_{m.app}$ values obtained at ten concentrations of aminoglycosides (between 0 and 20 μM) in MES buffer (24 mM).

Equations (1), (2) and (3) define the dependencies of the observed kinetic parameters on the concentrations of aminoglycosides (e.g., KanA) or aminosulfonates (e.g., MES):

$$k_{cat}^{obs} = \frac{k_{cat}^0 K_{d.ES} + k_{cat}^A [KanA]}{K_{d.ES} + [KanA]} \quad (1)$$

$$K_m^{obs} = \frac{K_{d.ES} K_m^0 \left(1 + \frac{[MES]}{K_I^0}\right) + K_m^A [KanA] \left(1 + \frac{[MES]}{K_I^A}\right)}{K_{d.ES} + [KanA]} \quad (2)$$

$$\left(\frac{k_{cat}}{K_m}\right)_{obs} = \frac{k_{cat}^0 K_{d.ES} \left(1 + \frac{[MES]}{K_I^A}\right) + \frac{k_{cat}^A [KanA]}{K_m^A}}{K_{d.E} \left(1 + \frac{[MES]}{K_I^0}\right) + [KanA] \left(1 + \frac{[MES]}{K_I^A}\right)} \quad (3)$$

X-ray crystallography: Crystallizations of His-tagged proteins were performed at 18 °C using hanging drops. The first crystal form (BlaKr) was obtained in the absence of kanamycin. The reservoir contained 500 μL solution (bis-tris buffer (0.1 M, pH 6.2), PEG 6000 (25% (*w/v*)), sodium azide (0.02% (*w/v*)) and sodium chloride (0.3 M)) in water. The hanging drop contained protein solution (1 μL) with reservoir solution (1 μL). Crystals appeared after a few days. For co-crystallization attempts in the presence of kanamycin, the composition of the reservoir aqueous solution contained MES buffer (0.1 M, pH 6.5), PEG 5000 MME (30% (*w/v*)) and ammonium sulfate (0.2 M). For the hanging drop, protein solution (0.5 μL containing 1 mM kanamycin) was mixed with reservoir solution (0.5 μL). Crystals ($BlaKrSO_4$) appeared after several weeks. In both cases, for data collection the crystals were flash cooled (100 K). The addition of a cryo-protectant was not necessary. The data were processed by XDS and XSCALE.[44] Both structures are orthorhombic, space group $P2_12_12_1$, with one molecule in the asymmetric unit (for data analysis, see the Supporting Information). The final coordinates and B-factors were deposited in the Protein Data Bank (IDs: 2v1z and 2v20). The residue numbering in the deposited structures is different from the conventional Ambler numbering[26] (conversion in Table S3).

ITC: Dialysed BlaKr solutions (0.07–0.15 mM) were titrated into the sample cell of a Microcal VP-ITC calorimeter (GE Healthcare) at 30 °C with ligand solutions (0.7–1.5 mM, pH 6.6). Titrations were performed with an injection volume of 4 μL for the first, and 10 μL for all subsequent titration points. Binding isotherms were analysed by MicrocalTM Origin 5.0 with models included in the software package. In each case, the first data point was discarded, and the baseline was adjusted manually. The integrated data were corrected for heat of the ligand dilution, as determined by the titration of the ligand into the buffer.

NMR spectroscopy: Fresh stock solutions of kanamycin sulfate (Roche) were prepared gravimetrically in the working buffers and stored at 4 °C. Prior to use, phenethylboronic acid was converted into the sodium salt by addition of an equimolar amount of NaOH to the working buffer; the pH was adjusted (6.60 ± 0.05 with concentrated HCl), and the resulting PhBA solution stored at 4 °C.

For backbone amide assignments of the free and PhBA-bound forms, two samples containing [U-^{13}C, U-^{15}N] BlaKr (0.6 mM in sodium phosphate (20 mM, pH 6.60)), with and without five molar equivalents of PhBA, were used. To transfer the assignments to the resonances of BlaKr in MES, 2D ^1H,^{15}N TROSY spectra were acquired of ^{15}N BlaKr (0.4 mM in MES (20 mM, pH 6.60)) in the presence of

sodium phosphate (0, 10, and 20 mM). For the NMR binding studies, ^{15}N BlaKr (0.3–0.5 mM in sodium phosphate (20 mM, pH 6.60) or MES (20 mM, pH 6.60)) was titrated with concentrated stock solutions of Kan or PhBA (10–20 mM) in the same buffer. The pH of the samples was checked during the titrations and, if necessary, adjusted to 6.60 ± 0.05 with 0.1 M HCl or NaOH. Measurements were performed at 30 °C on a DMX 600 MHz or Avancell 900 MHz spectrometer (Bruker Corporation, Billerica, MA), equipped with TCI-Z-GRAD or TCI 900S6 H-C/N-D-05 Z cryoprobes (Bruker), respectively. The binding of KanA and PhBA was followed in a series of 2D ^{1}H,^{15}N TROSY-HSQC spectra.[45] For further details, see the Supporting Information.

Acknowledgements

We thank Dr B. Granier and Dr J. Mareque Faez (Unisensor, Liège) for supplying biotinylated kanA, Prof. M. W. Makinen (University of Chicago) for his kind gift of the pET24(ompA) expression plasmid. A.N.V. acknowledges a fellowship from the Belgian "Inter-university Attraction Poles" program (P6/PROFUSA), financial support from the Belgian "Fonds de la Recherche Scientifique (F.R.S.-FNRS)" and Access to Research Infrastructures of the 6th EC Framework Program (contract # RII3–026145, EU-NMR). J.P.D. and C.E. acknowledge EC support for Access to the EMBL Hamburg Outstation, contract no. RII3-CT-2004–506 008, and to the ESRF BM30A beamline. We thank Stéphane Messe for performing the screening experiments, and Laurence Bausiers for expressing the BlaKr gene and purifying protein samples.

Keywords: allosteric regulation · antibiotics · beta-lactamases · directed evolution · kanamycin

[1] Q. Cui, M. Karplus, *Protein Sci.* **2008**, *17*, 1295 – 1307.
[2] N. M. Goodey, S. J. Benkovic, *Nat. Chem. Biol.* **2008**, *4*, 474 – 482.
[3] N. Ota, D. A. Agard, *J. Mol. Biol.* **2005**, *351*, 345 – 354.
[4] G. M. Süel, S. W. Lockless, M. A. Wall, R. Ranganathan, *Nat. Struct. Biol.* **2003**, *10*, 59 – 69.
[5] S. Brüschweiler, P. Schanda, K. Kloiber, B. Brutscher, G. Kontaxis, R. Konrat, M. Tollinger, *J. Am. Chem. Soc.* **2009**, *131*, 3063 – 3068.
[6] M. D. Sintchak, G. Arjara, B. A. Kellogg, J. Stubbe, C. L. Drennan, *Nat. Struct. Biol.* **2002**, *9*, 293 – 299.
[7] K. Kamata, M. Mitsuya, T. Nishimura, J. Eiki, Y. Nagata, *Structure* **2004**, *12*, 429 – 438.
[8] C. A. Brennan, K. Christianson, M. A. La Fleur, W. Mandecki, *Proc. Natl. Acad. Sci. USA* **1995**, *92*, 5783 – 5787.
[9] A. Benito, J. X. Feliu, A. Villaverde, *J. Biol. Chem.* **1996**, *271*, 21 251 – 21 256.
[10] N. Ferrer-Miralles, J. X. Feliu, S. Vandevuer, A. Müller, J. Cabrera-Crespo, I. Ortmans, F. Hoffmann, D. Cazorla, U. Rinas, M. Prévost, A. Villaverde, *J. Biol. Chem.* **2001**, *276*, 40087 – 40095.
[11] R. M. Ferraz, A. Vera, A. Aris, A. Villaverde, *Microb. Cell Fact.* **2006**, *5*, 1 – 7.
[12] D. Legendre, P. Soumillion, J. Fastrez, *Nat. Biotechnol.* **1999**, *17*, 67 – 72.
[13] G. Guntas, T. J. Mansell, J. R. Kim, M. Ostermeier, *Proc. Natl. Acad. Sci. USA* **2005**, *102*, 11224 – 11229.
[14] W. R. Edwards, K. Busse, R. K. Allemann, D. D. Jones, *Nucleic Acids Res.* **2008**, *36*, e78.
[15] A. R. Buskirk, Y.-C. Ong, Z. J. Gartner, D. R. Liu, *Proc. Natl. Acad. Sci. USA* **2004**, *101*, 10505 – 10510.
[16] G. Skretas, D. W. Wood, *Protein Sci.* **2005**, *14*, 523 – 532.
[17] J. Lee, M. Natarajan, V. C. Nashine, M. Socolich, T. Vo, W. P. Russ, S. J. Benkovic, R. Ranganathan, *Science* **2008**, *322*, 438 – 442.
[18] J. Fastrez, *ChemBioChem* **2009**, *10*, 2824 – 2835.
[19] A. Matagne, J. Lamotte-Brasseur, J.-M. Frère, *Biochem. J.* **1998**, *330*, 581 – 598.
[20] G. Zlokarnik, P. A. Negulescu, T. E. Knapp, L. Mere, N. Burres, L. Feng, M. Whitney, K. Roemer, R. Y. Tsien, *Science* **1998**, *279*, 84 – 88.
[21] S. Magnet, J. S. Blanchard, *Chem. Rev.* **2005**, *105*, 477 – 498.
[22] H. Watanabe, A. Satake, Y. Kido, A. Tsuji, *Analyst* **2002**, *127*, 98 – 103.
[23] E. E. M. G. Loomans, J. van Wiltenburg, M. Koets, A. van Amerongen, *J. Agric. Food Chem.* **2003**, *51*, 587 – 593.
[24] P. Mathonet, J. Deherve, P. Soumillion, J. Fastrez, *Protein Sci.* **2006**, *15*, 2323 – 2334.
[25] A. Petit, L. Maveyraud, F. Lenfant, J. P. Samama, R. Labia, J. M. Masson, *Biochem. J.* **1995**, *305*, 33 – 40.
[26] R. P. Ambler, A. F. W. Coulson, J.-M. Frère, J.-M. Ghuysen, B. Joris, M. Forsman, R. C. Levesque, G. Tiraby, S. G. Waley, *Biochem. J.* **1991**, *276*, 269 – 270.
[27] F. Rousseau, J. W. H. Schymkowitz, L. S. Itzhaki, *Structure* **2003**, *11*, 243 – 251.
[28] N. K. Vyas, *Curr. Opin. Struct. Biol.* **1991**, *1*, 732 – 740.
[29] W. I. Weis, K. Drickamer, *Annu. Rev. Biochem.* **1996**, *65*, 441 – 473.
[30] Commission Regulation (EC) no. 1140/1996. *Off. J. Eur. Communities: Legis*, L151.
[31] R. Martin, M. Gold, J. B. Jones, *Bioorg. Med. Chem. Lett.* **1994**, *4*, 1229 – 1234.
[32] C. Jelsch, L. Mourey, J. M. Masson, J.-P. Samama, *Protein J.* **1993**, *16*, 364 – 383.
[33] P.-Y. Savard, A. Sosa-Peinado, R. C. Levesque, M. W. Makinen, S. M. Gagné, *J. Biomol. NMR* **2004**, *29*, 433 – 434.
[34] P.-Y. Savard, S. M. Gagné, *Biochemistry* **2006**, *45*, 11414 – 11424.
[35] K. A. Schug, W. Lindner, *Chem. Rev.* **2005**, *105*, 67 – 114.
[36] A. Christensen, M. T. Martin, S. G. Waley, *Biochem. J.* **1990**, *266*, 853 – 861.
[37] J. Osuna, H. Viadiu, A. L. Fink, X. Soberón, *J. Biol. Chem.* **1995**, *270*, 775 – 781.
[38] P. Mathonet, H. Barrios, P. Soumillion, J. Fastrez, *Protein Sci.* **2006**, *15*, 2335 – 2343.
[39] J. R. Horn, B. K. Shoichet, *J. Mol. Biol.* **2004**, *336*, 1283 – 1291.
[40] V. J. Hilser, D. David, T. G. Oas, E. Freire, *Proc. Natl. Acad. Sci. USA* **1998**, *95*, 9903 – 9908.
[41] J. A. Hardy, J. A. Wells, *Curr. Opin. Struct. Biol.* **2004**, *14*, 706 – 715.
[42] A. Sosa-Peinado, D. Mustafi, M. W. Makinen, *Protein Expression Purif.* **2000**, *19*, 235 – 245.
[43] S. C. Gill, P. H. von Hippel, *Anal. Biochem.* **1989**, *182*, 319 – 326.
[44] W. Kabsch, *J. Appl. Crystallogr.* **1993**, *26*, 795 – 800.
[45] K. Pervushin, R. Riek, G. Wider, K. Wüthrich, *Proc. Natl. Acad. Sci. USA* **1997**, *94*, 12366 – 12371.
[46] W. L. DeLano, *The PyMOL Molecular Graphics System*, DeLano Scientific, Palo Alto, CA, USA, **2002**.

Received: September 21, 2010
Published online on ■■ ■■, 0000

Evolving regulation: An allosteric binding site for aminoglycoside antibiotics has been created in TEM1-β-lactamase by directed evolution. Aminoglycosides binding activates the enzyme by expulsion of an inhibitor, and allows their detection at low concentration. Interactions with several ligands offer opportunities for complex allosteric regulation.

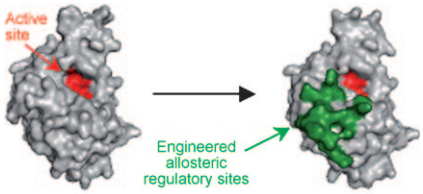

A. N. Volkov, H. Barrios, P. Mathonet, C. Evrard, M. Ubbink, J.-P. Declercq, P. Soumillion, J. Fastrez**

■■ – ■■

Engineering an Allosteric Binding Site for Aminoglycosides into TEM1-β-Lactamase

